

Age-related changes of the spinal cord: A biomechanical study

TOMOYA OKAZAKI¹, TSUKASA KANCHIKU¹, NORIHIRO NISHIDA¹,
KAZUHIKO ICHIHARA², ITSUO SAKURAMOTO³, JUNJI OHGI⁴, MASAHIRO FUNABA¹,
YASUAKI IMAJO¹, HIDENORI SUZUKI¹, XIAN CHEN⁴ and TOSHIHIKO TAGUCHI¹

¹Department of Orthopedic Surgery, Yamaguchi University Graduate School of Medicine, Ube, Yamaguchi 7558505;

²Non Profit Organization Corporation Japan Orthopedic Biomechanics Institute, Hofu, Yamaguchi 7470814; ³Department of Mechanical and Electrical Engineering, Tokuyama College of Technology, Gakuendai, Shunan, Yamaguchi 7458585;

⁴Department of Mechanical Engineering, Yamaguchi University, Ube, Yamaguchi 7558611, Japan

Received September 12, 2017; Accepted January 19, 2018

DOI: 10.3892/etm.2018.5796

Abstract. Although it is known that aging plays an important role in the incidence and progression of cervical spondylotic myelopathy (CSM), the underlying mechanism is unclear. Studies that used fresh bovine cervical spinal cord report the gray matter of the cervical spinal cord as being more rigid and fragile than the white matter. However, there are no reports regarding the association between aging and tensile and Finite Element Method (FEM). Therefore, FEM was used based on the data pertaining to the mechanical features of older bovine cervical spinal cord to explain the pathogenesis of CSM in elderly patients. Tensile tests were conducted for white and gray matter separately in young and old bovine cervical spinal cords, and compared with their respective mechanical features. Based on the data obtained, FEM analysis was further performed, which included static and dynamic factors to describe the internal stress distribution changes of the spinal cord. These results demonstrated that the mechanical strength of young bovine spinal cords is different from that of old bovine spinal cords. The gray matter of the older spinal cord was significantly softer and more resistant to rupture compared with that of younger spinal cords ($P < 0.05$). Among the old, although the gray matter was more fragile than the white matter, it was similar to the white matter in terms of its rigidity ($P < 0.05$). The *in vitro* data were subjected to three compression patterns. The FEM analysis demonstrated that the stress level rises higher in the old spinal cords in response to similar compression, when compared with young spinal cords. These results demonstrate that in analyzing the response of the spinal cord to compression, the age of patients is an

important factor to be considered, in addition to the degree of compression, compression speed and parts of the spinal cord compression factor.

Introduction

It is well known that the mobility of human beings declines with age. Nurick analyzed the natural process of cervical spondylotic myelopathy (CSM) and reported that aging affected the progress of symptoms (1). Although it is known that aging plays an important role in the incidence and progression of CSM, the underlying mechanism is unclear. There are studies that included Finite Element Method (FEM) from data obtained by experimenting with the gray and white matter of young bovine spinal cords (YBSC) (2). However, the application of their results may not be relevant in understanding CSM, a condition that usually occurs in the elderly (3-5). There are no studies that analyzed the *in-vitro* stress distribution within the spinal cord, or the mechanical properties of the spinal cord with respect to age.

In this study, we conducted tensile tests for bovine spinal cords of different ages, and performed an FEM of the data to investigate the effect of age on the response of the spinal cord to stress.

Materials and methods

Animals. The bovine were slaughtered at the Hofu city meat center. This institution is a licensed establishment. The animals were slaughtered from loss of blood. The experiment involved the use of bovine spongiform encephalopathy (BSE)-negative spinal cords that were sourced within 6 h of slaughter, and the experiment was completed within 10 h of slaughter. The spinal cords were sourced from two groups of animals, three young animals (YBSC; mean age, 46.3 ± 1.15 months) and three old animals [old bovine spinal cords (OBSC); mean age, 208 ± 14.8 months]. The specimens and instruments used for this experiment were under the instruction and supervision of the Hofu City Public Health Center and the Yamaguchi Prefecture Department of Sanitation. The Institutional Animal Care and Use Committee of Yamaguchi University waived requirement

Correspondence to: Dr Kazuhiko Ichihara, Non Profit Organization Corporation Japan Orthopedic Biomechanics Institute, 3-8-38 Mitajiri, Hofu, Yamaguchi 7470814, Japan
E-mail: biomechi@yamaguchi-u.ac.jp

Key words: degeneration, mechanical property, spinal cord, finite element method analysis, cervical spondilotic myelopathy

for ethical approval. Regulations of Yamaguchi University are subject to review researches using a living animals. This study used spinal cord of bovine that were slaughtered for food. Therefore, this study is excluded from the review.

Tensile test. Tensile tests for the YBSC and OBSC were conducted as described in previous studies (Fig. 1) (2,6). We removed the spinal cords carefully from bovine cervical spinal canal, and excised a 20-mm sample at the third cervical vertebral (C-3) (Fig. 1A). From this sample, longitudinal specimens of the white and gray matter (Fig. 1C) were prepared by using a bone marrow biopsy needle (internal diameter, 2.5 mm; Senko Ika Kogyo Co., Ltd, Japan) and a speed-gun (HS-2-12; Biomed-Instrumente Produkte GmbH, Germany) (Fig. 1B). The sampling positions were at the anterior horn of the gray matter and the lateral column of the white matter, respectively. We measured the diameter of the specimen at three points within a 10-mm long middle portion of the specimen by using a CCD Laser Micrometer (IG-010; KEYENCE, Tokyo, Japan) and calculated its surface area. Each end of the cylindrically-shaped specimen was fastened to two neoprene plates (each measuring 10x8x2 mm) with cyanoacrylate super-glue. These preparations were immediately inserted into the tension tester and testing was completed within 5 min of preparation of the samples. The room was humidified, and the temperature was maintained at 25°C to prevent the samples from drying. The specimens were elongated from the zero stress state, which was defined as the state wherein the initial length of the sample before elongation matched the contracted length after the removal of the spinal cord from the canal. The equipment for performing the tensile test included a high precision linear guide actuator (repeated positioning accuracy: ± 0.001 mm; THK Co., Ltd., Tokyo, Japan) and an alternating current servo motor (150 W, 1,500 rpm; Yasukawa Electronics, Tokyo, Japan). The deformation speed and tensile displacement were set by using the controller via a personal computer connected to an alternating current servo controller. A load cell (Microload Cells LVS-20GA; Kyowa Electronic Instruments, Tokyo, Japan; accuracy, 190 ± 0.53 mN) was attached to the actuator, and a gripping device was set on a movable table and the load cell. In the tensile test, the strain rate was fixed at 10 mm/sec, with the specimen being pulled at this rate till it ruptured. This test provided the stress-strain data by using three specimens from each animal.

FEM. The mechanical properties of the gray and white matters were determined by using the data obtained from the tensile tests with the 'least squares' method. The FEM model of the spinal cord was designed by using a software suite AbaqusV6.8 (Dassault Systemes Simulia Corp., Providence, RI, USA) and previous studies (6).

Since the structural elements in the spinal cord include the white matter, gray matter, dentate ligaments, and pia mater, the structural formula of each tissue type was introduced into the FEM model by using the hyper-elasticity and viscoelasticity characteristics obtained from the results of the tensile tests. In addition, we used 0.4 as the Poisson ratio for biological material. The FEM model has a total of 3,873 nodes and 3,762 elements. The anteroposterior diameter of the spinal cord was 10 mm in order to simplify calculation (Fig. 2A).

We set one rigid body at 25° in relation to the x-axis and assumed it to be the vertebral arch that formed the posterior boundary of the spinal cord. Dentate ligaments extend from the pia-mater covering the spinal cord to the spinal canal to provide fixation in the x- and y-axes. The posterior part of the spinal cord that touches the vertebral arch prior to any compression is fixed in the x- and y-axis.

Compression condition. For anterior compression, the rigid body, placed at 0° in relation to the x-axis, was allowed to compress the spinal cord along the y-axis anteroposteriorly, to simulate a bone spur. For posterior compression, a circular rigid body (diameter, 3 mm), placed at 65° in relation to the x-axis (to simulate a position vertical to the vertebral arch) was moved in a posteroanterior direction towards the center of the spinal cord. Since spinal cord disorders are caused by static and dynamic compression (2), we considered three models, chronic, acute, and acute-on-chronic compression for FEM (4). We set quasi-static compression speed at 0.008 m/s (based on the strain rate of a previously described tensile test (7)), and the dynamic compression speed at 2.22 m/s (based on the volunteer whiplash test result (8)). The total compression of the spinal cord for this model was set at 30% of diameter of spinal cord as suggested by a study on the pathology of cervical myelopathy (9). The type and quanta of compression applied in the different models were as follows: Chronic compression model, 30% quasi-static compression was applied from the anterior direction (Fig. 2B); acute compression model, 30% dynamic compression was applied from the anterior direction (Fig. 2B); Acute-on-chronic compression model: An initial 20% quasi-static compression was applied from the anterior direction, and then, followed by a 10% dynamic compression applied from the posterior direction (Fig. 2C).

Since allowable stress for each of the elements that compose the spinal cord is different, we first set the allowable stress point for each element with the assumption that irreversible damage would result in case this limit was exceeded. The ratio of the actual stress and the allowable stress for each part was displayed in red color whenever it exceeded one. A previous study demonstrated that axotomy of white matter occurs at an elongation of 0.28 (10). In this study, for a strain point of 0.28, white matter elongation was 0.015 MPa for YBSC and 0.046 MPa for OBSC. Another study demonstrated that the rapid rupture of gray matter is associated with allowable stress (4), and identified that the ruptured elongation of gray matter for YBSC was 0.386, and corresponded to a stress point of 0.092 MPa, while for OBSC, it was 0.59 and 0.060 MPa. We set the allowable stress points of the posterolateral sulcus (the most fragile part of the pia mater) and the dentate ligaments at 3.0 MPa and 18.7 MPa, respectively, based on previously (5). All statistical analysis were conducted using stat view version 5.0.

Result

Tensile test

Gray matter of OBSC and YBSC. In the elongation range 0.0-0.4, the stress amount and tangent modulus for YBSC were significantly higher than that for the OBSC ($P < 0.05$). However, beyond the 0.4, this was reversed and the values were

significantly higher for the OBSC ($P < 0.05$). The elongation at failure tended to be lower for YBSC ($P < 0.1$). Further, the tensile strength was higher in YBSC ($P < 0.05$) (Table I, Fig. 3A).

White matter of OBSC and YBSC. In the elongation range 0.4-0.6, the tangent modulus for OBSC was significantly higher than that for the YBSC ($P < 0.05$). However, there was no significant difference between the two groups in terms of the tangent modulus for elongation beyond this range, or at failure (Table I, Fig. 3B).

Tensile test: Analysis of tissue

White and gray matter of OBSC. In the elongation range between 0.0-0.1, and beyond 0.4, the tangent modulus of the white matter was significantly higher than that of the gray matter ($P < 0.05$). There was no difference in the tangent modulus of the two in the 0.1-0.4 range. The gray matter ruptured significantly earlier than the white matter ($P < 0.05$). Also, the tensile strength of the white matter was significantly higher ($P < 0.05$) (Table I, Fig. 3C).

White and gray matter of YBSC. The tangent modulus of the gray matter was significantly higher than that of the white matter at all strain rates ($P < 0.05$). The elongation at failure of the gray matter was significantly smaller than of the white matter ($P < 0.05$), although there was no significant difference in the tensile strength between the two (Table I, Fig. 3D).

FEM

Chronic compression model. The stress response of tissues following chronic compression was then investigated (Fig. 4). Anterior 1-mm compression: YBSC (Fig. 4Aa), OBSC (Fig. 4Ba); the stress in both the spinal cord models remained low.

Anterior 2-mm compression: In the YBSC, the parts of the white matter surrounding the anterior and posterior horn were identified as areas of mildly high stress distribution (Fig. 4Ab). In the OBSC, the gray matter was identified as an area of mildly high stress distribution. The white matter surrounding the gray matter was identified as an area of high stress distribution (Fig. 4Bb).

Anterior 3-mm compression: In the YBSC, the white matter around the gray matter was identified as an area of high stress distribution (Fig. 4Ac). In the OBSC, with the exception of a part of the posterior funiculus, the white and gray matter were all identified as areas of high stress distribution (Fig. 4Bc).

Acute compression model. Anterior 1-mm compression: In both the YBSC and OBSC, the anterior spinal cord was identified as an area of mildly high stress distribution (Fig. 4Ca and Da).

Anterior 2-mm compression: In the YBSC, a part of the anterior funiculus appeared as an area of mildly high stress distribution, while a part of the lateral funiculus appeared as an area of high stress distribution (Fig. 4Cb). In the OBSC, the posterior horn of the gray matter appeared as an area of high stress distribution. In addition, except anterior funiculus, all white matters surrounding the gray matter appeared as areas of high stress distribution (Fig. 4Db).

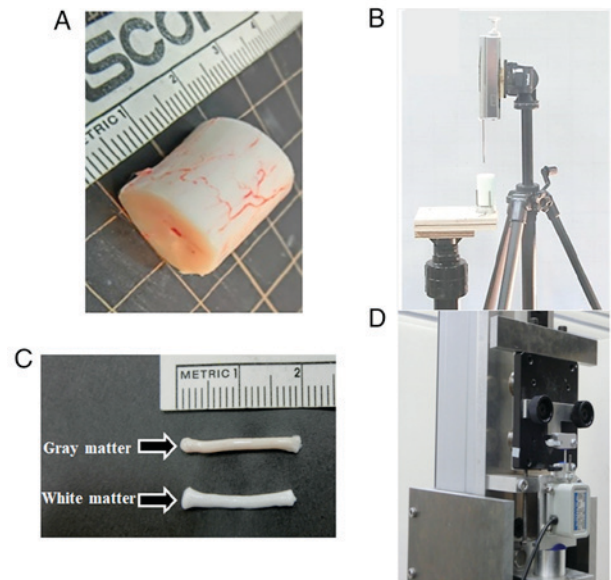


Figure 1. (A) Spinal cord cut into 20 mm sample. (B) Spinal cord tissue remover. (C) Removed specimen of the white and gray matter. (D) Equipment for the tensile test.

Anterior 3-mm compression: In the YBSC, the white matter around the gray matter was identified as an area of high stress distribution (Fig. 4Cc). The area of high stress distribution in the gray and white matter appeared to have expanded when compared to the chronic compression model. In the OBSC, with the exception of a part of the posterior funiculus, all the white and gray matter appeared as areas of high stress distribution (Fig. 4Dc).

Acute-on-chronic compression model. Anterior 2-mm and posterior 0.5-mm compression: In the YBSC, the stress over a part of the posterior horn and the posterior funiculus appeared to increase greatly (Fig. 4Eb). In the OBSC, the stress over a posterior horn and the posterior funiculus appeared to increase greatly (Fig. 4Fb).

Anterior 2-mm and posterior 1.0-mm compression: In YBSC, the stress over a part of the posterior horn, the posterior funiculus, and the lateral funiculus around the posterior horn increased (Fig. 4Ec). However, the stress in the anterior horn and the anterior funiculus decreased. In the OBSC, the stress over all areas of gray matter increased, while that over the white matter surrounding the gray matter increased greatly. The stress over the anterior funiculus was higher than that seen in the YBSC (Fig. 4F).

Discussion

It has been reported before, based on tensile tests conducted on the white and gray matter of YBSC that the gray matter of the cervical spinal cord was more rigid and fragile than the white matter. (2) A possible pathogenesis of CSM based on this FEM analyses has also been proposed (6,11-16). Although the analyses appeared to support other clinical reports, the study focused only on one physical property. This was because the data were obtained from experiments performed on the spinal cord of a young cow. It is possible that the mechanical

Table I. Results of the tensile test.

Tissue	Elongation at failure (kPa)	Tensile strength (kPa)	Tangent modulus (kPa)				
			0-0.1	0.1-0.2	0.2-0.4	0.4-0.6	0.6
Young gray matter (n=6)	0.386±0.0358	92.6±6.62	140±20.9	298±26.0	315±77.6	37.3±13.2	
Young white matter (n=8)	0.928±0.115 ^d	110±20.9	93.6±19.0 ^d	155±34.1 ^d	188±35.5 ^d	115±27.4 ^d	63.0±15.4
Old gray matter (n=6)	0.459±0.0733	60.2±30.5 ^b	33.2±14.6 ^b	70.6±30.8 ^b	206±74.7 ^b	98.0±92.2 ^b	
Old white matter (n=7)	0.852±0.293 ^c	112±41.2 ^c	65.4±32.5 ^c	113±52.9	171±33.1	229±54.2 ^{a,c}	79.2±31.9

Values are presented as the means ± standard deviation. ^aP<0.05 (Student's t-test) comparison with young white matter. ^bP<0.05 (Student's t-test) comparison with young gray matter. ^cP<0.05 (Student's t-test) comparison with old gray matter. ^dP<0.05 (Student's t-test) comparison with young gray matter.

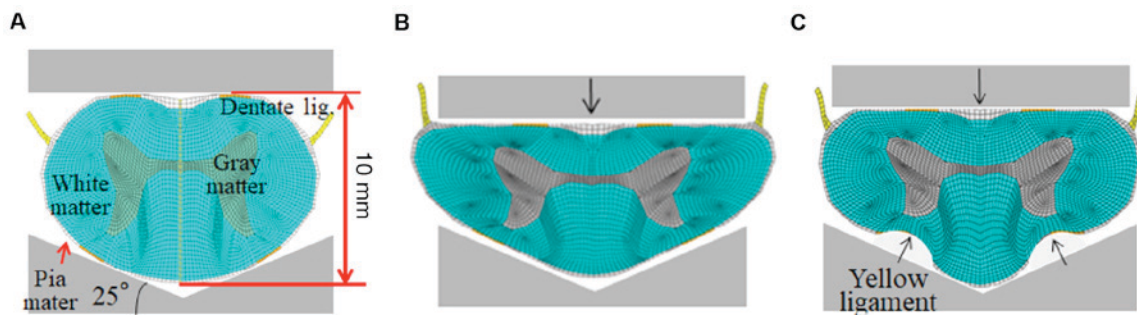


Figure 2. Finite Element Method analysis. (A) Before compression. (B) Anterior compression model and (C) anterior plus posterior compression model.

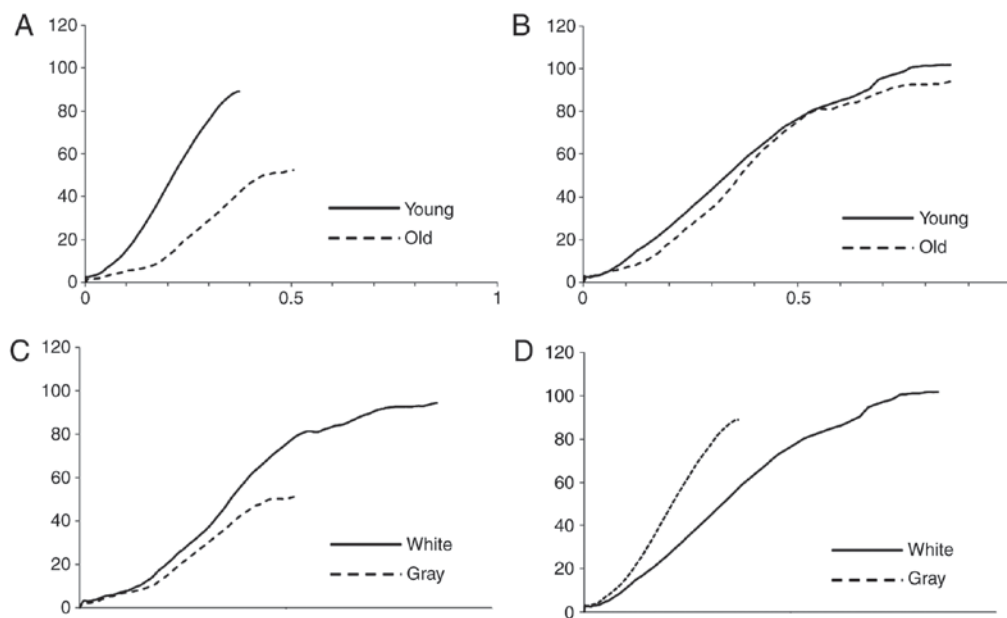


Figure 3. Result of tensile test. (A) Gray matter of old and young. (B) White matter of old and young. (C) Gray and white matter of old. (D) Gray and white matter of young.

performance of YBSC, and its analysis, may not be appropriate for understanding a condition like CSM, which is common in elderly. Therefore, we decided to perform a FEM of data obtained from the cervical cords of older animals.

In this study, we first compared the mechanical features of the gray and white matters of YBSC and OBSC by subjecting

them to tensile tests. We then designed FEM analysis of spinal cord compression by using the data derived from the tensile tests, to explain the mechanism of CSM.

The results of our study confirmed that mechanical strength for YBSC is different from that of OBSC, with the gray matter of the OBSC being softer, and with a reduced tendency to

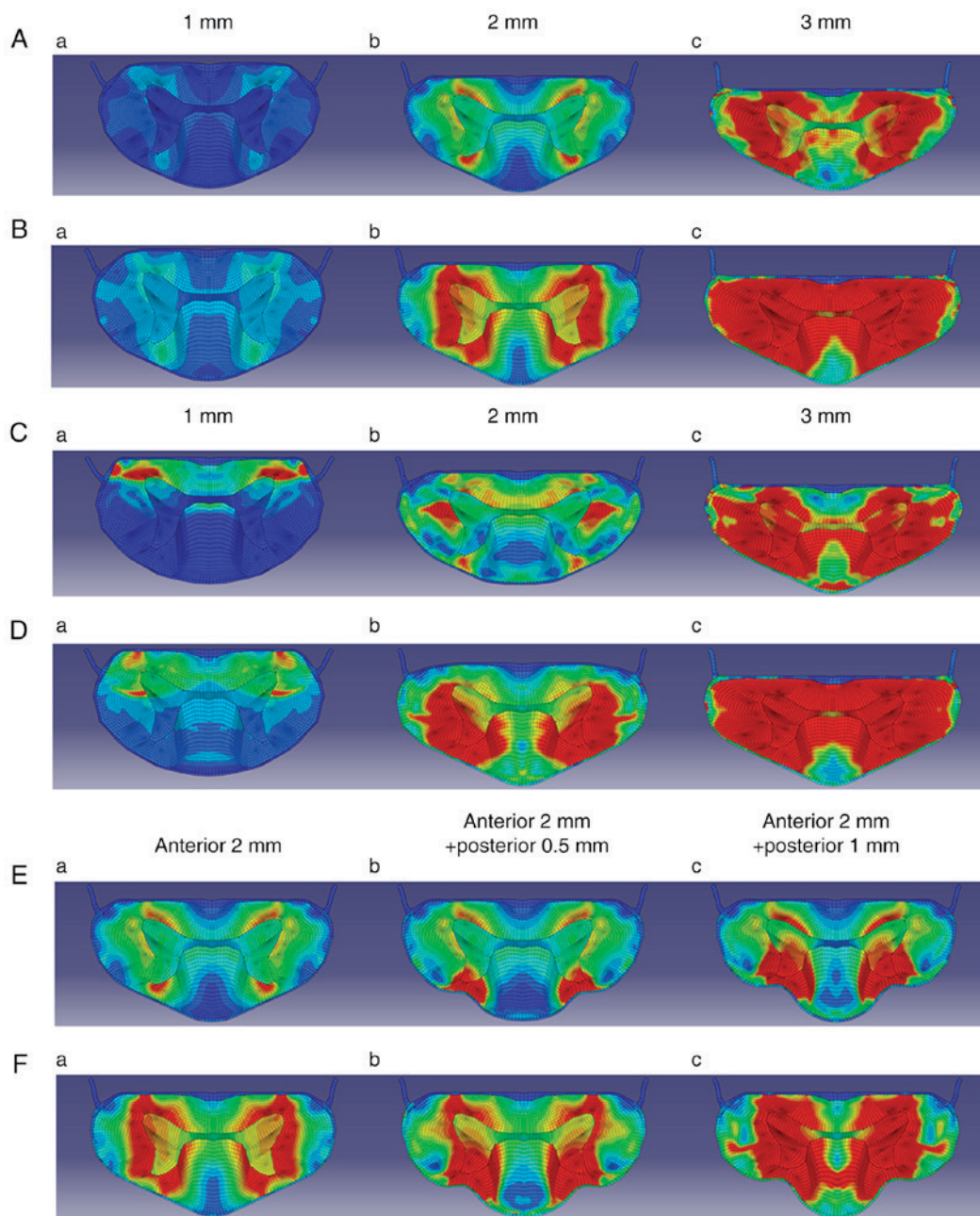


Figure 4. Result of Finite Element Method analysis. (A) Young chronic compression model. (B) Old chronic compression model. (C) Young acute compression model. (D) Old acute compression model. (E) Young chronic + acute compression model. (F) Old chronic + acute compression model.

rupture compared to the YBSC. Within the YBSC, the gray matter was harder and more fragile than the white matter. In the OBSC, although the gray matter was more fragile than the white matter, the rigidity of the gray and white matter was similar.

FEM was based on the results of the tensile tests, our analyses demonstrated that the stress distribution in the spinal cord of the old spinal cord model tended to rise earlier, when compared to the young spinal cord model.

There are no studies analyzing the difference in the physical properties between young and old spinal cords. However, several clinical reports suggested that the association between age and surgical outcomes. Suri *et al* demonstrated a difference in the rate of post-operative recovery between patients under, and above the age of 40 y (17). Similarly, Chagas *et al*

reported the association between age (at a cutoff of 60 y) (18). Nagashima *et al* identified that upper and lower extremity motor function tends to decrease with age (19). Nurick observed that CSM is more progressive among elderly patients than in touch that are younger (1).

It is unusual for the spinal cord to be subjected to external force in the absence of any compression. We established that aging is associated with a change in the physical property of bovine spinal cord. In this regard, our results corroborate with previous reports suggesting that elderly people tend to develop CSM, and have lower post-operative recovery rates. Our results suggest that the increase in stress levels in response to compression in older spinal cords occurs earlier than in younger spinal cords. A few studies demonstrated that the white and gray matter of the spinal cord undergo morphological changes

with age (20,21). Our results also indicate that the difference in the internal stress level between young and old bovine cover a broad range of symptom of CSM in elderly. Therefore, it is regarded as one of the reason that the diagnosis of CSM becomes difficult for the physical properties to participate.

Limitation

Our study had a few limitations. First, we extrapolated findings from a bovine experiment to explain a human condition. However, there are no prior studies demonstrating any correlation between human and bovine age. Second, we used only the tensile test results in designing the FEM model. Because tensile test is only way to demand a physical property. Future research may consider the use of compression tests as well. Although this study has such limitations, our study suggest that aging is associate with various symptoms of CSM in elderly. Our study demonstrated a difference in the physical properties of YBSC and OBSC. Additionally, FEM suggested a difference in the internal stress levels between the two. Elderly patients may develop CSM earlier than younger individuals even though they are exposed to a similar degree of compressive forces, mainly owing to age-related spinal cord degeneration. Further, even in conditions that expose the elderly to minor degree of compression, close monitoring is required as they are more likely to develop CSM.

Acknowledgements

We appreciate Mr. Ikuo Matsubayashi of Ginchiku Stock Farm Co. for his cooperation and generous gift of the bovine cervical spinal cords; Mr. Daigo Nakandakari and Mr. Tetsumi Fukumoto for his acquisition and analysis of data; Mr. Makoto Tamura and Mrs. Jennifer Tamura for assistance with the editing of this article.

References

1. Nurick S: The natural history and the results of surgical treatment of the spinal cord disorder associated with cervical spondylosis. *Brain* 95: 101-108, 1972.
2. Ichihara K, Taguchi T, Shimada Y, Sakuramoto I, Kawano S and Kawai S: Gray matter of the bovine cervical spinal cord was mechanically more rigid and fragile than the white matter. *J Neurotrauma* 18: 361-367, 2001.
3. Clarke E and Robinson PK: Cervical myelopathy: A complication of cervical spondylosis. *Brain* 79: 485-510, 1956.
4. Lees F and Turner JW: Natural history and prognosis of cervical spondylosis. *Br Med J* 2: 1607-1610, 1963.
5. Li XF and Dai LY: Acute central cord syndrome: Injury mechanisms and stress features. *Spine (Phila Pa 1976)* 35: E955-E964, 2010.

6. Ichihara K, Taguchi T, Sakuramoto I, Kawano S and Kawai S: Mechanism of the spinal cord injury and the cervical spondylotic myelopathy: New approach based on the mechanical features of the white and gray matter of the spinal cord. *J Neurosurg* 99 (3 Suppl): S278-S285, 2003.
7. Lebl DR, Hughes A, Cammisia FP Jr and O'Leary PF: Cervical spondylotic myelopathy: Pathophysiology, clinical presentation, and treatment. *HSS J* 7: 170-178, 2011.
8. Kaneoka K, Ono K, Inami S and Hayashi K: Motion analysis of cervical vertebrae during whiplash loading. *Spine* 24: 763-770, 1999.
9. Fujiwara K, Yonenobu K, Hiroshima K, Ebara S, Yamashita K and Ono K: Morphometry of the cervical spinal cord and its relation to pathology in cases with compression myelopathy. *Spine* 13: 1212-1216, 1998.
10. Galbraith JA, Thibault LE and Matteson DR: Mechanical and electrical responses of the squid giant axon to simple elongation. *J Biomech Eng* 115: 13-22, 1993.
11. Kato Y, Kataoka H, Ichihara K, Imajo Y, Kojima T, Kawano S, Hamanaka D, Yaji K and Taguchi T: Biomechanical study of cervical flexion myelopathy using a three-dimensional finite element method. *J Neurosurg Spine* 8: 436-441, 2008.
12. Kato Y, Kanchiku T, Imajo Y, Kimura K, Ichihara K, Kawano S, Hamanaka D, Yaji K and Taguchi T: Biomechanical study of the effect of degree of static compression of the spinal cord in ossification of the posterior longitudinal ligament. *J Neurosurg Spine* 12: 301-305, 2010.
13. Nishida N, Kato Y, Imajo Y, Kawano S and Taguchi T: Biomechanical analysis of cervical spondylotic myelopathy: The influence of dynamic factors and morphometry of the spinal cord. *J Spinal Cord Med* 35: 256-261, 2012.
14. Nishida N, Kanchiku T, Kato Y, Imajo Y, Yoshida Y, Kawano S and Taguchi T: Biomechanical analysis of cervical myelopathy due to ossification of the posterior longitudinal ligament: Effects of posterior decompression and kyphosis following decompression. *Exp Ther Med* 7: 1095-1099, 2014.
15. Nishida N, Kanchiku T, Imajo Y, Suzuki H, Yoshida Y, Kato Y, Nakajima D and Taguchi T: Stress analysis of the cervical spinal cord: Impact of the morphology of spinal cord segments on stress. *J Spinal Cord Med* 39: 327-334, 2016.
16. Nishida N, Kanchiku T, Kato Y, Imajo Y, Yoshida Y, Kawano S and Taguchi T: Cervical ossification of the posterior longitudinal ligament: Factors affecting the effect of posterior decompression. *J Spinal Cord Med* 40: 93-99, 2017.
17. Suri A, Chhabra RP, Mehta VS, Gaikwad S and Pandey RM: Effect of intramedullary signal changes on the surgical outcome of patients with cervical spondylotic myelopathy. *Spine J* 3: 33-45, 2003.
18. Chagas H, Dominques F, Aversa A, Vidal Fonseca AL and de Souza JM: Cervical spondylotic myelopathy: 10 years of prospective outcome analysis of anterior decompression and fusion. *Surg Neurol* 64 (Suppl 1): S30-S36, 2005.
19. Nagashima H, Morio Y, Yamashita H, Yamane K and Teshima R: Clinical features and surgical outcomes of cervical myelopathy in the elderly. *Clin Orthop Relat Res* 444: 140-145, 2006.
20. Kameyama T, Hashizume Y, Ando T, Takahashi A, Yanagi T and Mizuno J: Spinal cord morphology and pathology in ossification of the posterior longitudinal ligament. *Brain* 118: 263-278, 1995.
21. Nishida N, Kato Y, Imajo Y, Kawano S and Taguchi T: Biomechanical analysis of cervical spondylotic myelopathy: The influence of dynamic factors and morphometry of the spinal cord. *J Spinal Cord Med* 35: 256-261, 2012.



This work is licensed under a Creative Commons Attribution-NonCommercial-NoDerivatives 4.0 International (CC BY-NC-ND 4.0) License.